Graphic Abstract:

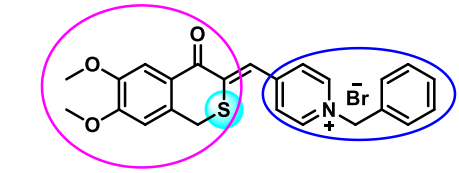

PAS of AChE

CAS of AChE

AChE: IC_{50} = 2.7 nM

No neurotoxicity at 50 μM

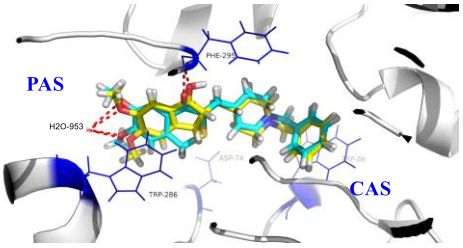

Dual-site AChE inhibitor

Design, Synthesis and Molecular Modeling of Isothiochromanone Derivatives as Acetylcholinesterase Inhibitors

Background: A series of novel isothio- and isoselenochromanone derivatives bearing *N*-benzyl pyridinium moiety were designed, synthesized and evaluated as acetylcholinesterase (AChE) inhibitors. **Results:** Most of the target compounds exhibited potent anti-AChE activities with IC_{50} values in nanomolar ranges. Among them, compound **15a** exhibited the most potent anti-AChE activity (IC_{50} = 2.7 nM), moderate antioxidant activity and low neurotoxicity. Moreover, the kinetic and docking studies revealed that compound **15a** was a mixed-type inhibitor, which bound to PAS and CAS of AChE. **Conclusion:** Those results suggested that compound **15a** might be a potential candidate for AD treatment.

Keywords: Alzheimer's disease; Acetylcholinesterase inhibitors; Isothiochromanone; Isoselenochromanone; Dual binding site

Alzheimer's disease (AD), characterized by dementia associated the loss of memory, cognitive and thinking, is a progressive neurodegenerative disease [1]. In 2018, it was estimated that over 47 million elderly people suffered from AD, and this number will be tripled by 2050 to 140 million [2]. Although considerable researches have been devoted to the pathogenetic mechanisms of AD, the etiology of AD still remains unclear. Several pathological hallmarks including amyloid-β (Aβ) deposits, reduction of acetylcholine (ACh), τ-protein aggregation, inflammation and oxidative stress, have been verified to be associated with the pathogenesis of AD [3]. At present, the clinical approach for AD therapy has focused on increasing the brain levels of acetylcholine in AD patients with acetylcholinesterase inhibitors (AChEIs), such as donepezil, rivastigmine and galantamine [4, 5]. Accordingly, based on the cholinergic hypothesis, the low level of acetylcholine results in cognitive and memory deficits,

and the improvement of the cholinergic function is an effective way to overcome the occurrence, symptoms and progression of AD [6].

The crystal structure of AChE has been reported [7]. It possesses a catalytic active site (CAS) at the bottom of the deep narrow gorge and a peripheral anionic site (PAS) near the entrance of gorge which could accelerate Aβ peptide deposition and promote the formation of Aβ fibril [8]. Therefore, designing the dual-site AChE inhibitors interacting with both the CAS and PAS are meaningful for AD prevention.

It was reported that the introduction of *N*-benzyl pyridinium moiety into aromatic scaffolds could endow them with potent AChE inhibitory activities, such as compounds **1-4** [9-12] (Figure 1). In our previous studies, a series of novel dual-site AChE inhibitors bearing the *N*-benzyl pyridinium moiety derived from natural product (±)-7, 8-Dihydroxy-3-methylisochroman-4-one [(±)-XJP] were designed and synthesized (Figure 2). The docking studies revealed that the presence of *N*-benzyl pyridinium moiety contributed to inhibition activities by interacting with the CAS of AChE, and the 4-isochromanone moiety formed stacking interactions with PAS of AChE [8]. To explore the effect of methoxy groups at 4-isochromanone skeleton on the AChE inhibitory activity, a series of derivatives have been further synthetized. The results showed that compound **6** exhibited the most potent anti-AChE activity and the highest AChE / BuChE selectivity with low neurotoxicity [13]. The structure-activity relationships (SARs) studies demonstrated compounds bearing methoxy group at both 6 and 7 positions exhibited more potent anti-AChE activity than those with methoxy group at other positions. Although, the preliminary SARs of the 4-isochromanone compounds bearing *N*-benzyl pyridinium moiety have been studied previously, the effect of the oxygen atom at the 4-isochromanone skeleton on the AChE inhibitory activity was undefined. According to previous reports, the compounds containing selenium and sulfur exhibits a wide range of bioactivity, especially for antioxidation and neuroprotection [14, 15]. Therefore, with the goal of discovering new anti-AChE agents with novel skeletons as well as completing the SARs of the isochromanone hybrids, we further designed and synthesized a series of isothio or isoselenochromanone derivatives by using bioisosterism strategy (Figure 2). Herein,

we would like to report their synthesis, AChE and BuChE inhibitory activities, antioxidant activity, the kinetic and molecular modeling studies.

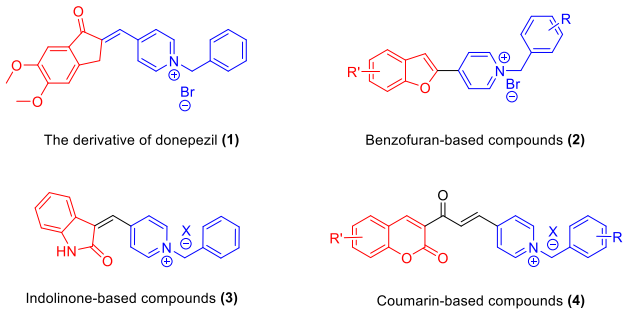

Figure 1. Some potent anti-AChE compounds bearing benzyl pyridinium moiety

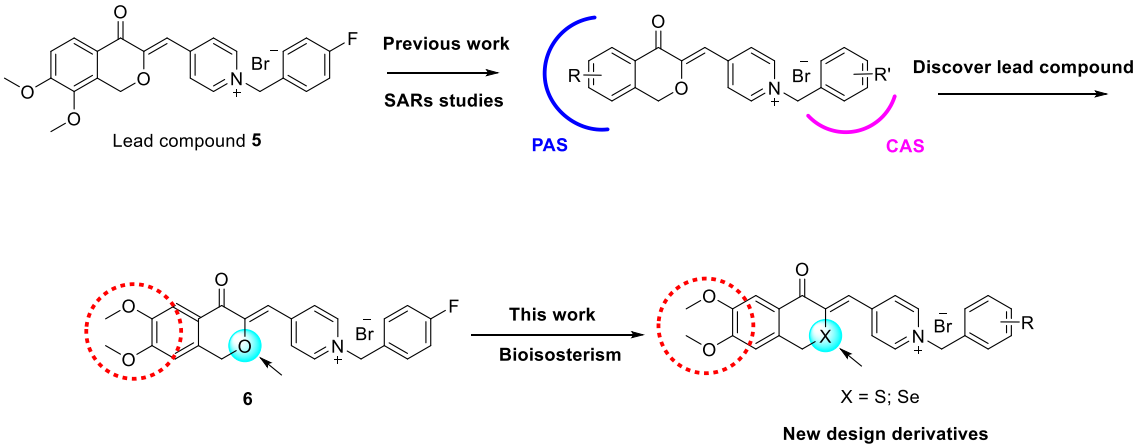

Figure 2. Design strategy of the target compounds

Materials & methods

Chemistry

All commercially available starting materials and solvents were reagent grade and used without further purification unless otherwise noted. ^{1}H NMR and ^{13}C NMR spectra were recorded on Bruker-300 spectrometers using $CDCl_3$ or DMSO-d_6 as solvent, and were referenced to the residual peaks of $CHCl_3$ at 7.26 ppm or DMSO-d_6 at 2.50 ppm (^{1}H NMR) and $CDCl_3$ at 77.23 ppm or DMSO-d_6 at 39.52 ppm (^{13}C NMR). Chemical shifts (δ) were reported in ppm using TMS as an internal standard. Coupling constants (J) are expressed in Hz and spin multiplicities are given as s (singlet), d (doublet), dd (doublet of doublets), and m (multiplet). HRMS was

performed on an Agilent 6530 Q-TOF mass spectrometer, and ESI-MS was carried out on an Agilent 6120 mass spectrometer. TLC was performed on Huanghai HSGF 254 silica gel plates (China). Silica gel 60 H (200-300 mesh), manufactured by Qingdao Haiyang Chemical Group Co., Ltd (China) was used for general chromatography.

The synthesis of intermediate 8.

To a solution of (3,4-dimethoxyphenyl)methanol (300 mg, 1.78 mmol) in 10 mL acetonitrile, trimethylsilyl chloride (339 μL, 2.68 mmol) and KI (444.14 mg, 2.68 mmol) were added and the mixture was stirred for 45 min at ambient temperature. Then the mixture was extracted with ethyl acetate (3 × 25 mL). The combined organic layers were then washed with brine (25 mL), dried over anhydrous Na_2SO_4, and concentrated in vacuo. The residues were purified by column chromatography with petroleum / ethyl acetate (10: 1) as eluent to afford 422.1 mg products **8** as yellow solids in 85.1% yields.

The synthesis of intermediate 9.

0.85 g (10.79 mmol) Se power was added into 20 mL deionized water at room temperature, and the mixture was stirred for 15 min. Sodium borohydride (612.19 mg, 16.18 mmol) in 20 mL of deionized water was slowly added into Se power suspension at room temperature. After the initial vigorous reaction had subsided (20 min), one additional equiv of Se powder (0.85 g, 10.79 mmol) was added and a brownish red solution was obtained. At room temperature, a solution of 4-(iodomethyl)-1, 2-dimethoxybenzene (3 g, 10.79 mmol) in 15 mL refined THF was added and the mixture was stirred for 30 min. Then the mixture was extracted with ethyl acetate (3 × 125 mL). The combined organic layers were then washed with brine (100 mL), dried over anhydrous Na_2SO_4, and concentrated in vacuo. The residues were purified by column chromatography with petroleum / ethyl acetate (4: 1) as eluent to afford 4.10 g **9** as yellow oil in 82.3% yields.

The synthesis of intermediate 10a.

To a solution of 4-(iodomethyl)-1,2-dimethoxybenzene (2.5 g, 8.99 mmol) in 40 mL acetone, ethyl 2-mercaptoacetate (1.18 mL, 10.79 mmol) and K_2CO_3 (1.86 g,

13.48 mmol) was added and the mixture was stirred for 5 h at room temperature. Then the mixture was extracted with ethyl acetate (3 × 125 mL). The combined organic layers were then washed with brine (100 mL), dried over anhydrous Na_2SO_4. The solvent was removed under reduced pressure to give yellow oil **10a**.

The synthesis of intermediate 10b.

Under N_2 atmosphere, to a solution of 1, 2-bis(3,4-dimethoxybenzyl)diselane (2g, 4.35 mmol) in 30 mL MeOH, $NaBH_4$ (246.57 mg, 6.52 mmol) was added and stirred for 20 min. Then ethyl 2-bromoacetate (2.4 mL, 6.52 mmol) was dropped in and the mixture was stirred for 1 h at room temperature. The reaction was quenched by water and the solvent was removed under reduced pressure. Then the mixture was extracted with ethyl acetate (3 × 125 mL). The combined organic layers were then washed with brine (100 mL), dried over anhydrous Na_2SO_4. The solvent was removed in vacuo to give yellow oil **10b**.

The synthesis of intermediates 11a and 11b.

To the solution of intermediate **10a** (2 g, 7.40 mmol) or **10b** (2 g, 6.30 mmol) in 20 mL MeOH, 5 mL 10% NaOH solution was dropped in and the mixture was stirred for 30 min at reflux temperature. The solvent was removed under reduced pressure. The residues were extracted with ethyl acetate (2 × 125 mL) to remove impurities. The water layer was first adjusted to pH 4, and after adding water (50 mL), it was extracted with ethyl acetate (3 × 125 mL). The combined organic layers were then washed with brine (100 mL), dried over anhydrous Na_2SO_4. The solvent was removed in vacuo to afford 1.55 g **11a** and 1.61 g **11b** as yellow oil with yields of 86.6% and 88.5%, respectively.

The synthesis of intermediates 12a and 12b.

To the solution of **11a** (2 g, 8.25 mmol) or **11b** (2 g, 6.92 mmol) in 20 mL dry dichloromethane, oxalyl dichloride (2 eq.) was added and the mixture was stirred for 30 min at 0 ℃. Then the solvent was removed under reduced pressure. The residues were dissolved in 10 mL chlorobenzene, then $SnCl_4$ (2 mL) was dropped in the solutions at 0 ℃ and the mixtures were stirred for 2 h at room temperature. The solvent was removed in vacuo. The residues were washed with saturated aqueous

solution of $NaHCO_3$ and the mixtures were diluted with 125 mL ethyl acetate. After filtering, the mixtures were washed with water (3 × 75 mL). The organic layers were then washed with brine (75 mL), dried over anhydrous Na_2SO_4, and concentrated in vacuo. The residues were purified by column chromatography with petroleum / ethyl acetate (10: 1; 4: 1) as eluent to afford **12a** or **12b** as white solid, yield 70.3% or 79.1%.

The synthesis of intermediates 13a and 13b.

To the solutions of **12a** (300 mg, 1.34 mmol) or **12b** (300 mg, 1.11 mmol) and pyridine-4-carboxaldehyde (1.2 eq.) in 2 mL DMF, 2 mL 10% K_2CO_3 aqueous solution was dropped in slowly at 0 ℃. After stirred for 30 s - 2 min at 0 ℃, the reactions appeared the precipitates and the water was added into the reactions. Then the precipitates were collected by filtration, washed with water and dried to afford **13a** and **13b** in general yields.

(*Z*)-6,7-dimethoxy-3-(pyridin-4-ylmethylene)isothiochroman-4-one (13a).

Yield 57.9%, yellow solid; ^{1}H NMR (300 MHz, $CDCl_3$) δ 8.66 (d, J = 6.2 Hz, 2H), 7.93 (s, 1H), 7.58 (s, 1H), 7.55 (d, J = 6.5 Hz, 2H), 6.68 (s, 1H), 3.96 (s, 6H), 3.95 (s, 2H); ^{13}C NMR (75 MHz, $CDCl_3$) δ 180.5, 153.1, 150.0, 149.0, 142.3, 134.0, 134.0, 131.8, 125.5, 124.0, 111.6, 109.3, 56.3, 56.2, 28.8; ESI-MS m/z 313.1 $[M+H]^+$ 314.1.

(*Z*)-6,7-dimethoxy-3-(pyridin-4-ylmethylene)isoselenochroman-4-one (13b).

Yield 62.3%, yellow solid; ^{1}H NMR (300 MHz, $CDCl_3$) δ 8.68 (d, J = 6.1 Hz, 2H), 8.24 (s, 1H), 7.53 (s, 1H), 7.44 (d, J = 6.2 Hz, 2H), 6.70 (s, 1H), 3.96 (s, 3H), 3.95 (s, 3H), 3.93 (s, 2H); ^{13}C NMR (75 MHz, $CDCl_3$) δ 182.0, 152.4, 150.1, 148.7, 143.4, 135.1, 134.6, 131.1, 126.8, 123.3, 112.4, 109.8, 56.2, 56.2, 20.8; ESI-MS m/z 361.0 $[M+H]^+$ 362.0.

The synthesis of intermediates 14a and 14b.

To a solution of **12a** (300 mg, 1.34 mmol) or **12b** (300 mg, 1.11 mg) in 10 mL THF, $NaOCH_3$ (3 eq.) was added at room temperature. After stirred for 30 s, the *N*-Boc-piperidine-4-carboxaldehyde (1.2 eq.) in THF (3 mL) was dropped in and the mixtures were stirred for 30 s - 2 min at room temperature. The mixtures were diluted with 10 mL water, then extracted with (3 × 25 mL) EtOAc. The combined organic

layers were then washed with brine (50 mL), dried over anhydrous Na_2SO_4 and concentrated in vacuo. The residues were dissolved in 10 mL DCM and CF_3COOH was added. After stirred for 2 h, the mixtures were diluted with 25 mL saturated $NaHCO_3$ solution and were extracted with DCM (3 × 25 mL). The combined organic layers were then washed with brine (50 mL), dried over anhydrous Na_2SO_4 and concentrated in vacuo. The residues were purified by column chromatography with petroleum / ethyl acetate (1: 1) as eluent to afford **14a** or **14b** in general yields.

(*Z*)-6,7-dimethoxy-3-(piperidin-4-ylmethylene)isothiochroman-4-one (14a).

Yield 60.2%, yellow oil; ^{1}H NMR (300 MHz, $CDCl_3$) δ 7.54 (s, 1H), 6.98 (d, J = 8.9 Hz, 1H), 6.63 (s, 1H), 5.03 (s, 1H), 3.92 (s, 2H), 3.90 (s, 3H), 3.86 (s, 3H), 3.47 (d, J = 13.1 Hz, 2H), 2.98 (s, 2H), 2.79 (s, 1H), 1.86 (d, J = 21.7 Hz, 4H); ^{13}C NMR (75 MHz, $CDCl_3$) δ 180.6, 152.8, 148.7, 140.0, 134.8, 130.8, 125.7, 111.5, 109.4, 56.2, 56.1, 43.4, 34.9, 29.7, 27.2; ESI-MS m/z 319.1 $[M+H]^+$ 320.1.

The synthesis of target compounds 15a – 15l.

Under N_2 atmosphere, to the solutions of 75 mg intermediate **13a**, **13b**, **14a** or **14b** in 8 mL acetonitrile, the proper benzyl bromide derivatives (1.1 eq.) and K_2CO_3 (1.5 eq.) were added and the mixtures were stirred for 1 - 2 h at reflux temperature. Then the solvents were removed in vacuo and the residues were purified by column chromatography with petroleum / ethyl acetate (2: 1) as eluent to afford **15e, 15f, 15k** or **15l** in general yields. And the residues were purified by column chromatography with DCM / MeOH (30: 1) as eluent to afford **15a - 15f** in low yields or **15g** – **15j** in general yields.

(*Z*)-1-benzyl-4-((6,7-dimethoxy-4-oxoisothiochroman-3

-ylidene)methyl)pyridin-1-ium bromide (15a).

Yield 30.2 %, red solid; ^{1}H NMR (300 MHz, DMSO-d_6) δ 9.22 (d, J = 6.5 Hz, 2H), 8.41 (d, J = 6.4 Hz, 2H), 7.96 (s, 1H), 7.61 – 7.54 (m, 2H), 7.50 (s, 1H), 7.48 – 7.46 (m, 1H), 7.45 (d, J = 4.7 Hz, 2H), 7.13 (s, 1H), 5.87 (s, 2H), 4.32 (s, 2H), 3.90 (s, 3H), 3.84 (s, 3H); ^{13}C NMR (75 MHz, DMSO-d_6) δ 178.5, 153.2, 150.2, 148.5, 144.4, 142.5, 134.7, 134.3, 129.3, 129.2, 128.8, 127.6, 125.8, 124.1, 110.8, 110.5, 62.7, 56.1,

55.7, 27.3; HR-MS (ESI) m/z: calcd for $C_{24}H_{22}BrNO_3S$ $[M\text{-}Br]^+$ 404.1315, found 404.1313.

(*Z*)-4-((6,7-dimethoxy-4-oxoisothiochroman-3-ylidene)methyl)-1-(4 fluorobenzyl)pyridin-1-ium bromide (**15b**).

Yield 31.3 %, red solid; ^{1}H NMR (300 MHz, DMSO-d_6) δ 9.18 (d, J = 6.5 Hz, 2H), 8.40 (d, J = 6.6 Hz, 2H), 7.96 (s, 1H), 7.70 – 7.59 (m, 2H), 7.44 (s, 1H), 7.36 – 7.26 (m, 2H), 7.13 (s, 1H), 5.83 (s, 2H), 4.32 (s, 2H), 3.90 (s, 3H), 3.84 (s, 3H); ^{13}C NMR (75 MHz, DMSO-d_6) δ 179.0, 164.7, 161.4, 153.7, 150.7, 149.0, 144.8, 143.0, 135.2, 132.0, 131.9, 131.1, 128.1, 126.3, 124.6, 116.8, 116.5, 112.0, 111.3, 111.0, 62.3, 56.6, 56.1, 27.8; HR-MS (ESI) m/z: calcd for $C_{24}H_{21}BrFNO_3S$ $[M\text{-}Br]^+$ 422.1221, found 422.1220.

(*Z*)-4-((6,7-dimethoxy-4-oxoisothiochroman-3-ylidene)methyl)-1-(3-fluorobenzyl) pyridin-1-ium bromide (**15c**).

Yield 29.7 %, red solid; ^{1}H NMR (300 MHz, DMSO-d_6) δ 9.21 (d, J = 6.5 Hz, 2H), 8.42 (d, J = 6.4 Hz, 2H), 7.97 (s, 1H), 7.50 (d, J = 9.2 Hz, 2H), 7.43 (d, J = 6.3 Hz, 2H), 7.27 (s, 1H), 7.13 (s, 1H), 5.86 (s, 2H), 4.32 (s, 2H), 3.90 (s, 3H), 3.84 (s, 3H)；HR-MS (ESI) m/z: calcd for $C_{24}H_{21}BrFNO_3S$ $[M\text{-}Br]^+$ 422.1221, found 422.1223.

(*Z*)-4-((6,7-dimethoxy-4-oxoisothiochroman-3-ylidene)methyl)-1-(2-fluorobenzyl) pyridin-1-ium bromide (**15d**).

Yield 33.1 %, red solid; ^{1}H NMR (300 MHz, DMSO-d_6) δ 9.13 (d, J = 6.5 Hz, 2H), 8.42 (d, J = 6.5 Hz, 2H), 7.97 (s, 1H), 7.67 – 7.62 (m, 1H), 7.56 – 7.52 (m, 1H), 7.45 (s, 1H), 7.35 (d, J = 6.9 Hz, 2H), 7.14 (s, 1H), 5.95 (s, 2H), 4.33 (s, 2H), 3.90 (s, 3H), 3.85 (s, 3H); ^{13}C NMR (75 MHz, DMSO-d_6) δ 179.0, 162.6, 159.3, 153.7, 151.0, 149.1, 145.1, 144.4, 143.2, 143.2, 135.2, 132.6, 132.5, 132.0, 128.0, 126.2, 125.8, 124.6, 121.8, 121.6, 116.6, 116.4, 111.3, 111.0, 57.8, 56.6, 56.2, 27.8; HR-MS (ESI) m/z: calcd for C24H21BrFNO3S $[M\text{-}Br]^+$ 422.1221, found 422.1228.

(*Z*)-3-((1-(3-fluorobenzyl)piperidin-4-yl)methylene)-6,7-dimethoxyisothiochroman-4-one (**15e**).

Yield 75.5 %, yellow solid; ^{1}H NMR (300 MHz, $CDCl_3$) δ 7.59 (s, 1H), 7.31 – 7.25 (m, 1H), 7.12 (d, J = 2.3 Hz, 1H), 7.09 (s, 1H), 7.07 (d, J = 2.3 Hz, 1H), 6.99 – 6.91

(m, 1H), 6.66 (s, 1H), 3.95 (s, 3H), 3.94 (s, 3H), 3.87 (s, 2H), 3.51 (s, 2H), 2.92 – 2.85 (m, 2H), 2.62 – 2.54 (m, 1H), 2.15 – 2.06 (m, 2H), 1.76 – 1.69 (m, 2H), 1.65 – 1.56 (m, 2H); ^{13}C NMR (75 MHz, $CDCl_3$) δ 180.8, 164.0, 160.8, 152.1, 148.1, 143.9, 140.8, 140.7, 134.5, 129.1, 129.0, 128.3, 125.6, 124.0, 124.0, 115.3, 115.1, 113.4, 113.2, 111.0, 108.8, 62.4, 55.7, 55.6, 52.6, 36.7, 30.2, 28.7; HR-MS (ESI) m/z: calcd for $C_{24}H_{26}FNO_3S$ $[M + H]^+$ 428.1690, found 428.1695.

(*Z*)-3-((1-(2-fluorobenzyl)piperidin-4-yl)methylene)-6,7-dimethoxyisothiochroman-4-one (**15f**).

Yield 77.1 %, yellow solid; ^{1}H NMR (300 MHz, $CDCl_3$) δ 7.57 (s, 1H), 7.42 – 7.36 (m, 1H), 7.26 – 7.20 (m, 1H), 7.13 (dd, J = 7.4, 1.3 Hz, 1H), 7.10 – 7.07 (m, 1H), 7.06 – 7.00 (m, 1H), 6.65 (s, 1H), 3.94 (s, 3H), 3.93 (s, 3H), 3.86 (s, 2H), 3.61 (s, 2H), 2.96 – 2.89 (m, 2H), 2.60 – 2.49 (m, 1H), 2.19 – 2.11 (m, 2H), 1.76 – 1.68 (m, 2H), 1.65 – 1.55 (m, 2H); ^{13}C NMR (75 MHz, $CDCl_3$) δ 181.3, 163.0, 159.8, 152.6, 148.6, 144.4, 135.0, 131.6, 131.6, 128.8, 128.7, 128.6, 126.1, 124.9, 124.7, 123.8, 123.8, 115.3, 115.0, 111.5, 109.3, 56.2, 56.1, 55.6, 52.8, 37.2, 30.7, 29.2; HR-MS (ESI) m/z: calcd for $C_{24}H_{26}FNO_3S$ $[M + H]^+$ 428.1690, found 428.1699.

(*Z*)-1-benzyl-4-((6,7-dimethoxy-4-oxoisoselenochroman-3-ylidene)methyl)pyridin-1-ium bromide (**15g**).

Yield 49.5 %, yellow solid; ^{1}H NMR (300 MHz, DMSO-d_6) δ 9.28 (s, 2H), 8.51 – 8.32 (m, 2H), 8.29 (s, 1H), 7.60 (s, 2H), 7.47 (s, 3H), 7.39 (s, 1H), 7.12 (s, 1H), 5.91 (s, 2H), 4.29 (s, 2H), 3.90 (s, 3H), 3.83 (s, 3H); ^{13}C NMR (75 MHz, DMSO-d_6) δ 180.5, 152.5, 151.3, 148.3, 144.5, 140.5, 135.5, 134.2, 130.0, 129.3, 129.2, 128.9, 127.2, 125.5, 111.7, 110.9, 62.7, 56.1, 55.7, 20.9; HR-MS (ESI) m/z: calcd for $C_{24}H_{22}BrNO_3Se$ $[M\text{-}Br]^+$ 452.0759, found 452.0754.

(*Z*)-4-((6,7-dimethoxy-4-oxoisoselenochroman-3-ylidene)methyl)-1-(4 fluorobenzyl)pyridin-1-ium bromide (**15h**).

Yield 50.2 %, yellow solid; ^{1}H NMR (300 MHz, $CDCl_3$) δ 9.57 (d, J = 6.2 Hz, 2H), 8.09 (s, 1H), 8.06 (d, J = 6.0 Hz, 2H), 7.87 – 7.76 (m, 2H), 7.44 (s, 1H), 7.08 – 6.99 (m, 2H), 6.80 (s, 1H), 6.29 (s, 2H), 4.10 (s, 2H), 3.97 (s, 3H), 3.92 (s, 3H);^{13}C NMR (75 MHz, DMSO-d_6) δ 181.0, 164.7, 161.4, 153.0, 151.9, 148.8, 144.9, 141.1, 135.9,

132.1, 131.9, 130.9, 130.9, 130.4, 127.7, 126.0, 116.8, 116.5, 112.2, 111.4, 62.4, 56.6, 56.2, 21.4; HR-MS (ESI) m/z: calcd for $C_{24}H_{21}BrFNO_3Se$ $[M-Br]^+$ 470.0665, found 470.0668.

(*Z*)-4-((6,7-dimethoxy-4-oxoisoselenochroman-3-ylidene)methyl)-1-(3 fluorobenzyl)pyridin-1-ium bromide (**15i**).

Yield 48.9 %, yellow solid; ^{1}H NMR (300 MHz, DMSO-d_6) δ 9.27 (d, J = 6.3 Hz, 2H), 8.36 (d, J = 6.2 Hz, 2H), 8.30 (s, 1H), 7.54 (d, J = 8.8 Hz, 2H), 7.49 – 7.42 (m, 1H), 7.40 (s, 1H), 7.32 (d, J = 8.9 Hz, 1H), 7.13 (s, 1H), 5.92 (s, 2H), 4.30 (s, 2H), 3.91 (s, 3H), 3.84 (s, 3H); ^{13}C NMR (75 MHz, DMSO-d_6) δ 181.1, 153.0, 152.0, 152.0, 148.8, 145.1, 141.2, 136.0, 136.0, 132.0, 131.8, 130.4, 127.7, 126.0, 125.6, 125.5, 116.9, 116.7, 116.6, 116.3, 116.2, 115.9, 112.2, 111.4, 62.5, 56.6, 56.2, 21.4; HR-MS (ESI) m/z: calcd for $C_{24}H_{21}BrFNO_3Se$ $[M-Br]^+$ 470.0665, found 470.0665.

(*Z*)-4-((6,7-dimethoxy-4-oxoisoselenochroman-3-ylidene)methyl)-1-(2-fluorobenz yl)pyridin-1-ium bromide (**15j**).

Yield 51.5 %, yellow solid; ^{1}H NMR (300 MHz, DMSO-d_6) δ 9.16 (d, J = 6.4 Hz, 2H), 8.35 (d, J = 6.4 Hz, 2H), 8.29 (s, 1H), 7.71 – 7.62 (m, 1H), 7.59 – 7.51 (m, 1H), 7.42 – 7.35 (m, 2H), 7.33 (d, J = 7.7 Hz, 1H), 7.12 (s, 1H), 5.97 (s, 2H), 4.29 (s, 2H), 3.90 (s, 3H), 3.83 (s, 3H); ^{13}C NMR (75 MHz, DMSO-d_6) δ 181.0, 162.6, 159.4, 153.0, 152.0, 148.8, 145.2, 141.4, 136.0, 132.7, 132.6, 132.0, 130.4, 127.7, 126.7, 126.1, 126.0, 125.8, 121.8, 121.6, 116.7, 116.4, 112.2, 111.4, 57.9, 56.6, 56.1, 21.4; HR-MS (ESI) m/z: calcd for $C_{24}H_{21}BrFNO_3Se$ $[M-Br]^+$ 470.0665, found 470.0674.

(*Z*)-3-((1-(3-fluorobenzyl)piperidin-4-yl)methylene)-6,7-dimethoxyisoselenochro man-4-one (**15k**).

Yield 79.5 %, yellow solid; ^{1}H NMR (300 MHz, $CDCl_3$) δ 7.53 (s, 1H), 7.32 – 7.24 (m, 2H), 7.11 – 7.03 (m, 2H), 6.97 – 6.89 (m, 1H), 6.66 (s, 1H), 3.94 (s, 3H), 3.92 (s, 3H), 3.85 (s, 2H), 3.50 (s, 2H), 2.92 – 2.84 (m, 2H), 2.46 – 2.34 (m, 1H), 2.12 – 2.03 (m, 2H), 1.72 – 1.65 (m, 2H), 1.65 – 1.54 (m, 2H); ^{13}C NMR (75 MHz, $CDCl_3$) δ 181.9, 164.0, 160.8, 151.5, 147.9, 146.3, 140.8, 140.7, 134.9, 129.1, 129.0, 126.9, 124.8, 124.0, 124.0, 115.3, 115.1, 113.5, 113.2, 111.9, 109.3, 62.3, 55.6, 52.5, 39.1, 30.1, 29.2, 20.0; HR-MS (ESI) m/z: calcd for $C_{24}H_{26}FNO_3Se$ $[M+H]^+$ 476.1135,

found 476.1136.

(*Z*)-3-((1-(2-fluorobenzyl)piperidin-4-yl)methylene)-6,7-dimethoxyisoselenochroman-4-one (**15l**).

Yield 78.8 %, yellow solid; ^{1}H NMR (300 MHz, $CDCl_3$) δ 7.52 (s, 1H), 7.42 – 7.35 (m, 1H), 7.28 (d, J = 8.6 Hz, 1H), 7.26 – 7.19 (m, 1H), 7.14 – 7.08 (m, 1H), 7.07 – 6.99 (m, 1H), 6.66 (s, 1H), 3.94 (s, 3H), 3.92 (s, 3H), 3.85 (s, 2H), 3.60 (d, J = 1.5 Hz, 2H), 2.97 – 2.89 (m, 2H), 2.44 – 2.32 (m, 1H), 2.18 – 2.09 (m, 2H), 1.72 (dd, J = 13.2, 3.7 Hz, 2H), 1.66 – 1.54 (m, 2H); ^{13}C NMR (75 MHz, $CDCl_3$) δ 182.5, 163.1, 159.8, 152.0, 148.4, 146.9, 135.4, 131.7, 131.6, 128.8, 128.7, 127.4, 125.3, 124.8, 123.9, 123.8, 115.4, 115.0, 112.3, 109.8, 100.0, 56.1, 56.1, 55.6, 52.7, 39.6, 30.6, 20.5; HR-MS (ESI) m/z: calcd for $C_{24}H_{26}FNO_3Se$ $[M+H]^+$ 476.1135, found 476.1142.

AChE and BuChE inhibitory activity test assay

Test samples were dissolved in DMSO as stock solutions of 10 mM and were diluted with buffer A to the proper concentration, and the concentration of DMSO in the solution did not exceeded 1%. In the 96-well plates, 30 μL of thioiodoacetylcholine (2 mM), 50 μL of AChE (0.22 U/mL, prepared with Buffer B) and 10 μL of different concentrations of inhibitors were mixed. The contents were incubated at 37 °C for 5 min, and then 30 μL of thioiodoacetylcholine (2 mM) was added to the mixture. After 1 min and 8 min, the reactions were terminated by 3 % SDS. The 160 μL of 0.2 % DTNB which was color agent was added. The linear increase in absorbance at 440 nM was measured after 0, 60, 120 and 180 s of incubation time. BuchE inhibition was assayed according to the similar method of AChE inhibition with minor modifications. Briefly, AChE needed to replace with BuChE (0.12 U/mL, prepared with Buffer B) and substrate iodoacetylcholine needed to replace with thioiodobenzoyl chloride (15 mM), other experimental conditions remain unchanged.

Cell viability

SH-SY5Y cells were planted in a 15 mL culture flask in Eagle's minimum essential medium (EMEM) and Ham's F-12 medium, supplemented with 10% fetal bovine serum, 100 U/mL penicillin and 100 μg/mL streptomycin, and the culture flask was

cultured in the incubator (37 ℃, 5% CO_2). The cells were then grown at 10^4 cells for per well in 96-well plates. When the cells were fused, the cells were placed in serum-free medium. The different concentrations of compounds **15a** and **15h** (1, 10, 50 μM) were added to the serum-free medium which cultured for 24 h in the incubator, then 10 μL of MTT was added at 37 °C. After cultured for 3 h, 100 μL of DMSO was added to dissolve methanine crystals at the end, and the absorbance the mixture was determined at 490 nM by microplate reader.

Kinetic study of AChE inhibition

To obtain the mechanism of **15a**, a series of experiments were performed by using Ellman's method as same as AChE assay. **15a** with concentration of 1.25 and 2.5 nM were selected for the kinetic analysis. Lineweaver-Burk reciprocal plots were constructed by plotting the 1 / velocity versus 1 / [substrate] at different concentration of substrate acetylthiocholine (0.05-0.5 mM) to obtain the type of inhibition. Data analysis was performed with GraphPad Prism 4.03 software.

***In vitro* antioxidant activity assay**

1,1-diphenyl-2-picryl-hydrazyl (DPPH) is commercially available organic nitrogen radicals which was used for the determination of free radical-scavenging activity of compounds **15a** and **15h**. The DPPH was dissolved in methanol to obtain a 0.1 mM concentration of DPPH stock solution. The 10 μL of the test samples at 100 μM and 90 μL of DPPH solution were added to 96-well plates. After reacting for 30 min at 25 ℃, the absorbance was recorded at 517 nM. And the trolox was applied as a reference.

Molecular modeling

In our study, the X-ray structure of the donepezil - AChE complex was downloaded from the Protein Data Bank (PDB code: 4ey7). The protein was prepared using Schrodinger. The docking procedure was performed by employing the Glide module in the Schrodinger software package, and the structural image was obtained using PyMOL software.

***In silico* ADMETox study**

An *in silico* study of synthesized compounds **15a–15l** was performed for

prediction of ADME properties and toxicity. For this purpose, Blood–brain barrier (BBB) permeability, human intestinal absorption (HIA), Caco2 permeability (Caco2) and some toxicity risk parameters were calculated by using online admetSAR.

Results & discussions

Chemistry

The synthetic route of the target compounds was shown in Figure 3. The iodination of the starting material **7** gave the intermediate **8** [16], which was substituted by ethyl 2-mercaptoacetate in the presence of K_2CO_3 to afford intermediate **10a**. The intermediate **9** was prepared by the reaction of intermediate **8** with newly prepared sodium selenide (Na_2Se_2), which was reduced by sodium borohydride ($NaBH_4$) in MeOH and treated with ethyl 2-bromoacetate to give the intermediate **10b** [17]. The intermediates **10a** and **10b** were hydrolyzed to give the corresponding acids **11a** and **11b**, which were then cyclized via Friedel-crafts reactions to give isothiochromanone **12a** and isoselenochromanone **12b**. Then, the key intermediates **12a** and **12b** reacted with pyridine-4-carboxaldehyde in the presence of 10% K_2CO_3 solution to give intermediates **13a** and **13b**. Intermediates **14a** and **14b** were synthesized by the similar methods using sodium methoxide as the base. Finally, compounds **13a**, **13b, 14a** and **14b** reacted with different benzyl bromide derivatives to yield the target compounds **15a - 15l**.

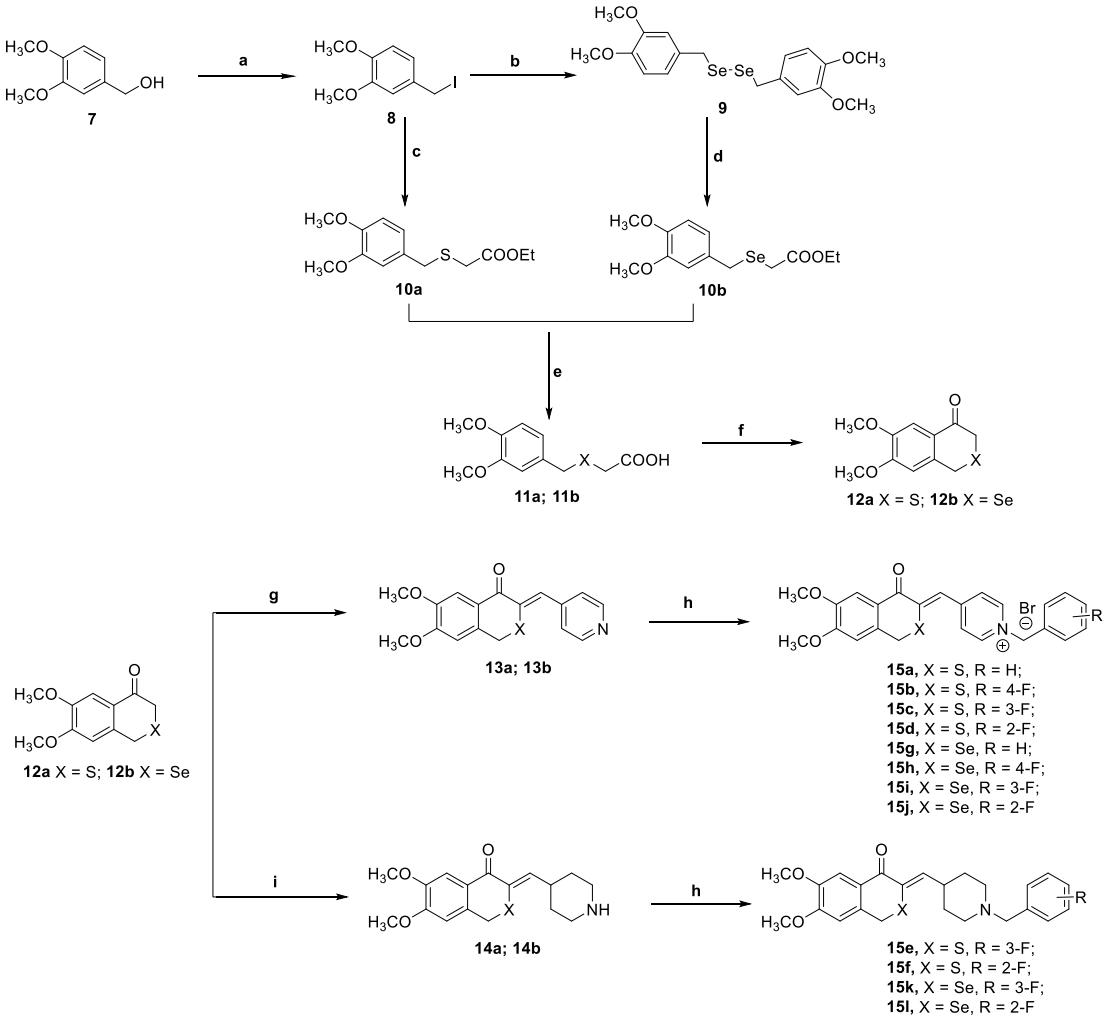

Figure 3. Reagents and conditions: (a) TMSCl, KI, CH_3CN, rt, 45 min; (b) Se, $NaBH_4$, H_2O, rt, 30 min; (c) ethyl 2-mercaptoacetate, K_2CO_3, acetone, rt, 5 h; (d) ethyl 2-bromoacetate, $NaBH_4$, MeOH, 3 h; (e) 10% NaOH solution, MeOH, 80 ℃, 30 min; (f) i) oxalyl dichloride, DCM, 0 ℃, 30 min; ii) $SnCl_4$, chlorobenzene, rt, 2 h; (g) isonicotinaldehyde, K_2CO_3, H_2O - DMF, 0 ℃, 30 s - 2 min; (h) proper benzyl bromide derivatives, MeCN, reflux, 1 - 2 h; (i) i) $NaOCH_3$, *N*-Boc-piperidine-4-carboxaldehyde, THF, rt, 1 - 5 min; ii), CF_3COOH, DCM, rt, 2 h.

In vitro inhibitory activity of cholinesterase

The inhibitory activity of all target compounds against AChE and BuChE were evaluated using the spectrophotometric method of Ellman *et al*. And donepezil was used as a reference [18]. The IC_{50} values for the inhibition of AChE and BuChE were presented in Table 1. The results revealed that all target compounds bearing *N*-benzyl pyridinium moiety exhibit significant inhibitory activity towards AChE with IC_{50} values in the nanomolar range, indicating that these compounds are potent AChE

inhibitors. However, the AChE inhibitory activity of compounds **15e**, **15f**, **15k** and **15l** decreased significantly when pyridine was changed to piperidine, suggesting that the *N*-benzyl pyridinium moiety is crucial for AChE inhibition. The unsubstituted benzyl pyridinium compound **15a** bearing an isothiochromanone moiety displayed the most potent inhibition against AChE with the IC_{50} value of 2.7 nM, which was 4.7-fold more potent than the positive control donepezil. The *para*-F substituted benzyl pyridinium compound **15h** bearing isoselenochromanone moiety also displayed a potent inhibitory activity (IC_{50} = 5.8 nM), which was 2.2-fold more potent than donepezil. Thus, the potent AChE inhibitory activity of this class of derivatives prompted us to further investigate their kinetic and binding modes.

Table 1. Inhibition of AChE and BuChE activities of the target compounds

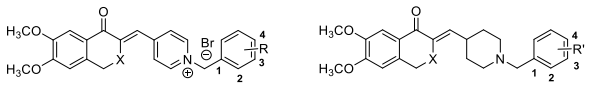

Compd.	R	R’	X	IC_{50} (means ± SEM) [a]	
				AChE (nM)	BuChE (nM)
15a	H	-	S	2.7 ± 0.08	440 ± 180
15b	4-F	-	S	11.9 ± 0.6	1440 ± 75
15c	3-F	-	S	18.4 ± 0.8	2079 ± 102
15d	2-F	-	S	9.8 ± 0.5	1480 ± 69
15e	-	3-F	S	7470 ± 323	N.D [b]
15f	-	2-F	S	8020 ± 356	N.D
15g	H	-	Se	9.9 ± 0.6	564 ± 31
15h	4-F	-	Se	5.8 ± 0.3	609 ± 33
15i	3-F	-	Se	11.9 ± 0.6	1059 ± 51
15j	2-F	-	Se	9.6 ± 0.5	931 ± 45
15k	-	3-F	Se	16400 ± 817	N.D
15l	-	2-F	Se	15600 ± 781	N.D
Donepezil	-	-	-	12.7 ± 0.5	737 ± 37

[a] IC_{50}: 50% inhibitory concentration (means ± SEM of three experiments).

[b] Not Determined.

Kinetic study of AChE inhibition

In order to analyze the AChE inhibitory mechanism of these inhibitors, the most potent compound **15a** was selected for a kinetic test. The type of inhibition was elucidated from the analysis of Lineweaver–Burk reciprocal plots (Figure 4), which showed both increasing slopes and intercepts on the y-axis with increasing concentration of inhibitor. According to this pattern, compound **15a** is a mixed-type inhibitor for AChE, which showed that compound **15a** might be able to simultaneously bind to the CAS and PAS of AChE.

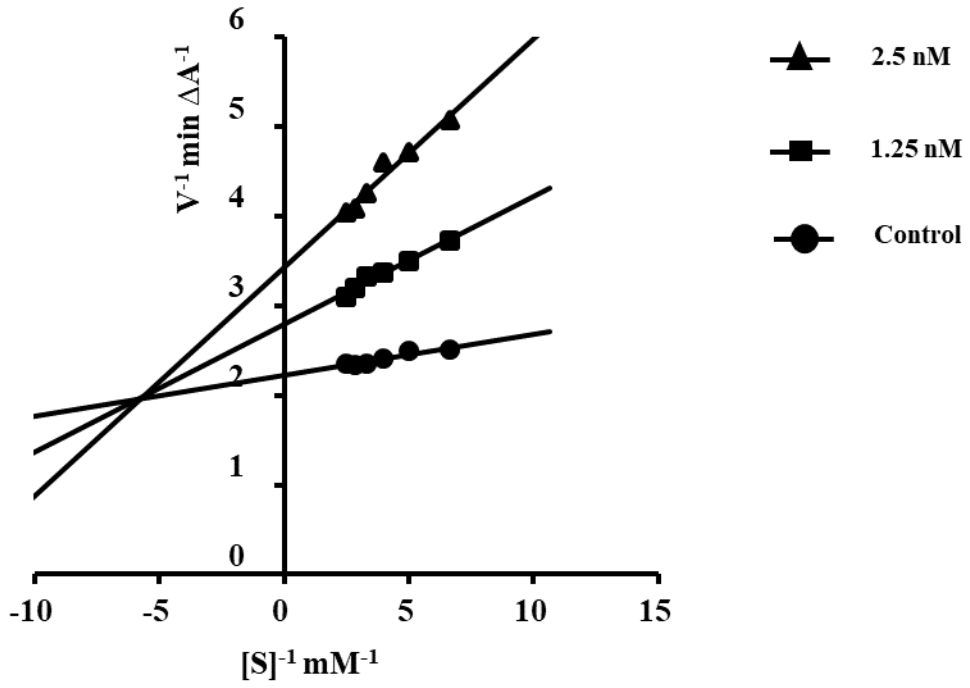

Figure 4. Lineweaver-Burk plots resulting from subvelocity curve of AChE activity with different substrate concentrations in the absence and presence of **15a** (0, 1.25, and 2.5 nM).

Cell viability assay of compounds 15a and 15h

To evaluate the cytotoxic effect of target compounds against nerve cell [19], the viability of SH-SY5Y cells treated with representative compounds **15a** and **15h** at different concentrations was determined. As shown in Table 2, negligible cytotoxicity was noted for compounds **15a** and **15h** at concentrations of 1 and 10 μM. When the

concentration rose to 50 μM, the survival rate only decreased slightly (> 80%) and the morphology of the SH-SY5Y cells was not affected, which indicated that compounds **15a** and **15h** have low neurotoxicity.

Table 2. Cell viability of compounds **15a** and **15h** on nerve cells SH-SY5Y.

Compounds	Concentrations (μM)	Cell viability (%)
15a	1	99.6 ± 0.5
	10	94.4 ± 0.9
	50	88.7 ± 4.5
15h	1	97.7 ± 0.7
	10	95.2 ± 0.7
	50	82.2 ± 0.8

***In vitro* antioxidant activity**

The radical scavenging activity of compounds **15a** and **15h** was determined by using 1,1-diphenyl-2-picryl-hydrazyl (DPPH) assay and trolox was used as a reference. The results showed that compounds **15a** and **15h** at a concentration of 100 μM possessed moderate antioxidant activity. The free radical scavenging activity of compounds **15a** and **15h** were 55% and 45% compared to trolox, respectively, which were more potent than that of compound **6** (10%).

Docking studies

To further explore the binding mode of compounds **15a** and **15h** with AChE, a molecular docking study was performed by using the Glide module in the Schrodinger software package. The X-ray crystal structure of AChE complexed with donepezil (PDB: 4ey7) was chosen as the docking protein. As shown in Figure 5, the overlay of the best poses of docked compounds **15a** and **15h** with donepezil in the active site clearly demonstrated that compounds **15a** and **15h** adopt similar dual-binding modes to that of donepezil in the binding pocket. As presented, the methoxy groups and

carbonyl group of isothio- and isoselenochromanone moieties formed three hydrogen bonds with a water molecule (H2O953) and the residue Phe295 of PAS, respectively. Isothio- and isoselenochromanone moieties showed π - π stacking interactions with Trp286, which is another important amino acid residue of PAS. In addition, the *N*-benzyl pyridinium moiety of compounds **15a** and **15h** bound to the CAS of AChE via aromatic π - π stacking interactions and salt bridge with Trp86 and Asp74, respectively. All these results indicated that compounds **15a** and **15h** could simultaneously bind to the PAS and CAS of AChE, which is in accordance with the results of kinetic study.

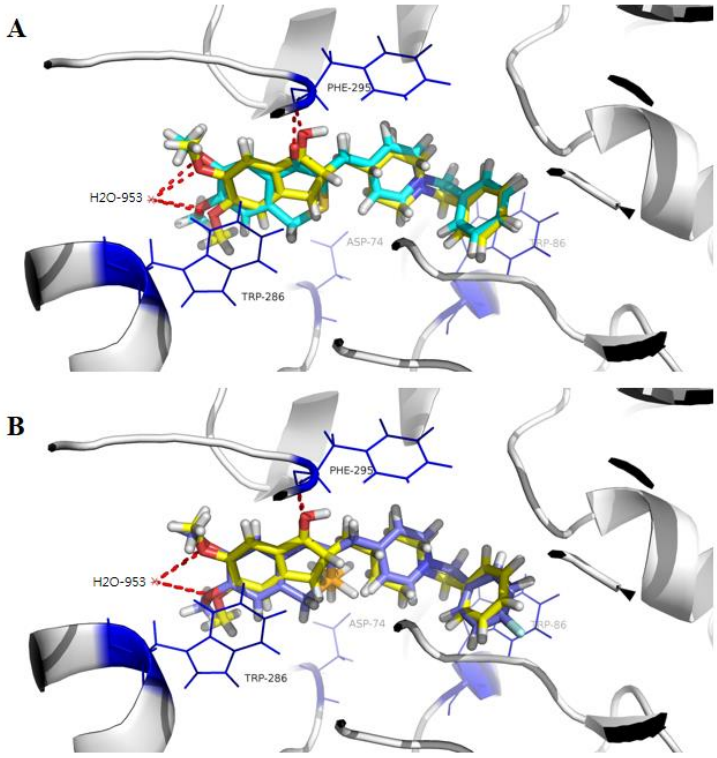

Figure 5. A) The docking mode of compound **15a** (cyan) and donepezil (yellow) with AChE; B) The docking mode of compound **15h** (purple) and donepezil with AChE. The hydrogen bonds of ligands with the target were shown by red dashed line.

Prediction of toxicity risks and drug-likeness properties

To evaluate the drug-likeness character of the target compounds, toxicity risks (mutagenicity, tumorigenicity, irritation, and reproduction) were predicted by Osiris calculation. Moreover, the ADME (Absorption, Distribution, Metabolism, and

Excretion) properties of the target compounds, such as BBB (Blood–Brain Barrier) penetration, HIA (Human Intestinal Absorption), Caco-2 cell permeability were also calculated using admetSAR web-based application [20]. As shown in Table 3, compounds **15a-f** bearing isothiochromanone moiety were predicted to be without toxicity risks, whereas compounds **15g-l** bearing isoselenochromanone moiety were tumorigenic. According to the predicted values for BBB, all compounds might be able to penetrate into the central nervous system (CNS). In the case of HIA and Caco-2 permeability, all compounds might be well absorbed from intestine.

Table 3. Osiris calculations and ADMET properties prediction of all compounds and donepezil.

Compd.	Toxicity Risks [a]				ADMET properties		
	MUT	TUM	IRRIT	RE	BBB [b]	HIA [c]	Caco-2 [d]
15a					+	+	+
15b					+	+	+
15c					+	+	+
15d					+	+	+
15e					+	+	+
15f					+	+	+
15g					+	+	+
15h					+	+	+
15i					+	+	+
15j					+	+	+
15k					+	+	+
15l					+	+	+
donepezil					+	+	+

[a] MUT: mutagenic; TUM: tumorigenic; IRRIT: irritant; RE: reproductive effective, green represents non-toxic and red represents toxic.

[b] Blood Brain Barrier. The values more than 95 was considered as +.

[c] Human Intestinal Absorption. The values more than 90 was considered as +.

[d] The values more than 50 was considered as +.

Conclusion

In conclusion, on the basis of our previous studies, twelve novel AChE inhibitors bearing *N*-benzyl pyridinium moiety derived from natural product XJP were further designed and synthesized. Most of the target compounds possessed potent AChE inhibitory activity. Among the synthesized compounds, compound **15a** displayed the most potent anti-AChE activity (IC_{50} = 2.7 nM), moderate antioxidant activity and low neurotoxicity. Moreover, according to the kinetic and docking studies, compound **15a** was proved to be a mixed-type inhibitor binding to the PAS and CAS of AChE. All these results highlighted **15a** was a promising lead compound for the development of anti-AD agents.

Future perspective

Alzheimer disease (AD), which has become a health problem worldwide, is the most common form of dementia in elderly people. However, the pathogenesis of AD still remains unclear. And the approved drug (donepezil, rivastigmine, galantamine and memantine) could only enable a palliative treatment instead of curing or preventing AD. Therefore, it is necessary to develop new and more effective anti-AD drugs.

Based on the results of our studies, most of the isothio- and isoselenochromanone derivatives were potent AChE inhibitors. Therefore, we speculate that isothio- and isoselenochromanone are desirable skeletons which could provide new insights into the development of anti-AD drugs.

Executive summary

Introduction:

● Alzheimer's disease (AD), which emerged as the main cause of dementia, has affected over 46 million elderly people in the worldwide.

Experimental section:

● A series of novel isothio- and isoselenochromanone derivatives were

designed, synthesized and evaluated as acetylcholinesterase (AChE) inhibitors.

Results & discussion:

● Most of target compounds bearing *N*-benzyl pyridinium moiety exhibited significant inhibitory activity compared with the positive donepezil.

● The docking and kinetic studies revealed that the most potent compound **15a** could bind to the PAS and CAS of AChE.

Conclusion:

● The results suggested that there is a great potential of isothio- and isoselenochromanone skeletons as the leads for further structural modification to develop new agents in treatment of AD.

Ethical conduct of research

The authors state that they have obtained appropriate institutional review board approval or have followed the principles outlined in the Declaration of Helsinki for all human or animal experimental investigations. In addition, for investigations involving human subjects, informed consent has been obtained from the participants involved.

References

Papers of special note have been highlighted as:

• of interest •• of considerable interest

1 Zhang C, Du Q, Chen L *et al*. Design, synthesis and evaluation of novel tacrine-multialkoxybenzene hybrids as multi-targeted compounds against Alzheimer's disease. *Eur. J. Med. Chem*. 116, 200-209 (2016).

2 Zhang P, Xu S, Zhu Z, Xu J. Multi-target design strategies for the improved treatment of Alzheimer's disease. *Eur. J. Med. Chem*. DOI: 10.1016/j.ejmech.2019.05.020 (2019).

3 Schelterns P, Feldman H. Treatment of Alzheimer's disease: current status and new perspectives. *Lancet Neurol*. 2 (9), 539-547 (2003).

4 Digiacomo M, Chen Z, Wang S *et al*. Synthesis and pharmacological evaluation of

multifunctional tacrine derivatives against several disease pathways of AD. *Bioorg. Med. Chem. Lett*. 25 (4), 807-810 (2015).

5 Singh M, Silakari O. Design, synthesis and biological evaluation of novel 2-phenyl-1-benzopyran-4-one derivatives as potential poly-functional anti-Alzheimer's agents. *RSC Adv.* 6 (110), 108411-108422 (2016).

6 Cai P, Fang S, Yang H *et al*. Donepezil-butylated hydroxytoluene (BHT) hybrids as anti-Alzheimer's disease agents with cholinergic, antioxidant, and neuroprotective properties. *Eur. J. Med. Chem*. 157, 161-176 (2018).

7 Xie S, Wang X, Li J, Yang L, Kong L. Design, synthesis and evaluation of novel tacrine–coumarin hybrids as multifunctional cholinesterase inhibitors against Alzheimer's disease. *Eur. J. Med. Chem*. 64, 540-553 (2013).

8 Wang C, Wu Z, Cai H *et al*. Design, synthesis, biological evaluation and docking study of 4-isochromanone hybrids bearing *N*-benzyl pyridinium moiety as dual binding site acetylcholinesterase inhibitors. *Bioorg. Med. Chem. Lett*. 25 (22), 5212-5216 (2015).

• **Design of the isochromanone hybrids as novel skeleton for AD treatment.**

9 Lan J, Zhang T, Liu Y *et al*. Design, synthesis and biological activity of novel donepezil derivatives bearing *N*-benzyl pyridinium moiety as potent and dual binding site acetylcholinesterase inhibitors. *Eur. J. Med. Chem*. 133, 184-196 (2017).

•• **Introducing the importance of *N*-benzyl pyridinium moiety in design of anti-AD agents.**

10 Baharloo F, Moslemin MH, Nadri H *et al*. Benzofuran-derived benzylpyridinium bromides as potent acetylcholinesterase inhibitors. *Eur. J. Med. Chem*. 93, 196-201(2015).

11 Akrami H, Mirjalili BF, Khoobi M *et al*. Indolinone-based acetylcholinesterase inhibitors: synthesis, biological activity and molecular modeling. *Eur. J. Med. Chem*. 84 (18), 375-381 (2014).

12 Alipour M, Khoobi M, Foroumadi A *et al*. Novel coumarin derivatives bearing *N*-benzyl pyridinium moiety: potent and dual binding site acetylcholinesterase inhibitors. *Bioorg. Med. Chem*. 20 (24), 7214-7222 (2012).

13 Wang J, Wang C, Wu Z *et al*. Design, synthesis, biological evaluation and docking study of 4-isochromanone hybrids bearing *N*-benzyl pyridinium moiety as dual binding site acetylcholinesterase inhibitors (Part II). *Chem. Biol. Drug. Des***.** 91, 756-762 (2018).

14 Wu J, Ling J, Wang X *et al.* Discovery of a potential anti-ischemic stroke agent: 3-pentylbenzo[c]thiophen-1(3H)-one. *J. Med. Chem*. 55, 7173-7181 (2012).

15 Luo Z, Sheng J, Sun Y *et al.* Synthesis and evaluation of multi-target-directed ligands against Alzheimer's disease based on the fusion of donepezil and ebselen. *J. Med. Chem*. 56, 9089-9099 (2013).

16 Sakai T, Miyata K, Utaka M, Takeda A. Me_3SiCl - NaI - CH_3CN as an efficient and practical reducing agent for benzylic alcohols. *Tetrahedron Lett.* 28(33), 3817-3818 (1987).

17 Bari SS, Bhalla A, Nagpal Y, Mehta SK, Bhasin KK. Synthesis and characterization of novel trans-3-benzyl / (diphenyl)methyl / naphthyl seleno substituted monocyclic β-lactams: X-ray structure of trans-1-(4'-methoxyphenyl)-3-(diphenyl)methylseleno-4-(4'-methoxyphenyl)azetidin-2-one. *J. Organomet. Chem.* 695 (17), 1979-1985 (2010).

18 Ellman GL, Courtney KD, Jr AV, Featherstone RM. A new and rapid colorimetric determination of acetylcholinesterase activity. *Biochem. Pharmacol.* 7 (2), 88 (1961).

- **The most important report describing the assay of cholinesterase activity**

19 Rizzo S, RivièRe C, Piazzi L *et al*. Benzofuran-Based hybrid compounds for the inhibition of cholinesterase activity, β amyloid aggregation, and Aβ neurotoxicity. *J. Med. Chem.* 51 (10), 2883-2886 (2008).

20 Cheng F, Li W, Zhou Y *et al*. admetSAR: a comprehensive source and free tool for assessment of chemical ADMET properties. *Chem. Inf. Model.* 52, 3099 – 3015 (2012).